Self-Assembled Polyaniline Nanostructures with Photoisomerization Function

Kun Huang and Meixiang Wan*

Center for Molecular Sciences, Institute of Chemistry, Chinese Academy of Sciences, Beijing 100080, P. R. China

Received February 11, 2002. Revised Manuscript Received April 24, 2002

Nanostructures (e.g., nanotubes and nanofibers) of polyaniline (PANI) with an average diameter of 110−130 nm and a conductivity of 2.5×10^{-2} S/cm were synthesized by a self-assembly process in the presence of azobenzenesulfonic acid (ABSA) as a dopant. It was found that the formation probability and size of PANI−ABSA nanostructures depended on the molar ratio of aniline to ABSA and the concentration of ABSA. ABSA or aniline−ABSA salt micelles were proposed to interpret the formation of PANI−ABSA nanostructures. In particular, the PANI−ABSA nanostructures exhibited trans−cis photoisomerization similar to that of the azobenzene moiety upon irradiation with UV light ($\lambda = 365$ nm).

Introduction

Azobenzene and its derivatives are generally characterized by reversible transformations from the more stable trans state to the less stable cis form upon irradiation with UV light.[1] Moreover, the photoinduced isomerization of the azobenzene moiety is accompanied by a structural change, as reflected by changes in the dipole moment and geometry.[2] In addition, because azobenzene can be selectively attached to the side chains, main chains, cross-links, or chain ends of a polymer, it can be used as a "photochromic" probe to construct new polymers with photochromic characteristics. In particular, the photochromic characteristic might provide light control of the chemical functions through an "on−off light switch". Thus, reports of azobenzene-functionalized polymers as potential materials for reversible optical storage media,[3] holographic gratings,[4] optical s,[5] and electrooptic modulators[6] have been published in the literature.

Among polymers, conducting polymers are a new generation of polymers because they cover the full range from insulator to metal and retain the attractive mechanical properties as well as processing advantages of polymers.[7,8] Recently, a few papers on conducting polymers containing the azobenzene moiety have been reported in the literature. Chen et al.,[9] for instance, reported that copolymers of 3-hexylthiophene and azobenzene-modified 3-hexylthiophene showed photo-controlled conductivity switching behavior, which was attributed to the generation of a photoexictation in the azobenzene moiety upon irradiation by UV light. Moreover, Yoshino et al.[10] also reported that poly(*p*-phenylenevinylene) (PPV) and polyacetylene (PA) derivatives including azobenzene moieties as side chains showed optical anisotropy accompanied by trans−cis isomerization of azobenzene upon irradiation by linearly polarized light. However, no papers dealing with conducting polymers including the azobezene moiety as a dopant have yet been published.

Currently, there is considerable interest in nanoscale materials because of their unique properties and promising potential applications in nanodevices such as nanowires,[11] sensor/actuator arrays,[12,13] and optoelectric devices,[14,15] as well as in biotechnology[16,17] (e.g., delivery agents for pharmaceutical agents). Template synthesis is a common and effective method for synthesizing these nanostructures of conducting polymers,[18−25] but post-

* To whom correspondence should be addressed. E-mail: wanmx@infoc3.icas.ac.cn.

(1) Humar, G. S.; Neckers, D. C. *Chem. Rev.* **1989**, *89*, 1915.
(2) Zimmerman, G.; Chow, L.; Paik, U. *J. Am. Chem. Soc.* **1958**, *80*, 3528.
(3) (a) Eich, M.; Wendorff, J. H. *J. Opt. Soc. Am. B* **1990**, *7*, 1428. (b) Ikeda, I.; Tsutusumi, O. *Science* **1995**, *268*, 1873.
(4) (a) Rochon, P.; Batalla, E.; Natanshon, A. *Appl. Phys. Lett.* **1995**, *66*, 136. (b) Kim, D. Y.; Li, L.; Kummar, J.; Tripathy, S. K. *Appl. Phys. Lett.* **1995**, *66*, 1166.
(5) Lückemeyer, T.; Francke, H. *Appl. Phys. Lett.* **1988**, *53*, 2017.
(6) Seki, T.; Skuragi, M.; Kawanishi, Y.; Suzuki, Y.; Tamiki, T.; Fukuda, R.; Ichimura, K. *Langmuir* **1993**, *9*, 211.
(7) Heeger, J. *Rev. Mod. Phys.* **2001**, *73*, 681.
(8) Skotheim, T. A.; Elsenbaumer, R. L.; Reyholds, J. F., Eds. *Handbook of Conducting Polymers*, 2nd ed.; Marcel Dekker: New York, 1998.
(9) Chen, S.-A.; Liao, C.-S. *Makromol. Chem., Rapid Commun.* **1993**, *14*, 69.
(10) Matsui, T.; Nagata, T.; Ozaki, M.; Fujii, A.; Onoda, M.; Teraguchi, M.; Masuda, T.; Yoshino, K. *Synth. Met.* **2001**, *119*, 599.
(11) Li, W. Z.; Xie, S. S.; Qian, L. X.; Chang, B. H.; Zhou, B. S.; Zhou, W. Y.; Zhao, R. A.; Wang, G. *Science* **1996**, *274*, 1701.
(12) Lindner, E.; Cosofret, V. V.; Ulfer, S.; Buck, R. P. *J. Chem. Soc., Faraday Trans.* **1993**, *89*, 361.
(13) Sakai, H.; Baba, R.; Hashimoto, K.; Fujishma, A. *J. Phys. Chem.* **1995**, *99*, 11896.
(14) Trau, M.; Yao, N.; Kim, E.; Xia, Y.; Whitesides, G. M.; Aksay, I. A. *Nature* **1997**, *390*, 674.
(15) Fendler, J. H. *Chem. Mater.* **1996**, *8*, 1616.
(16) Lasic, D. D. *Liposomes: From Physics to Applications*; Plenum Press: New York, 1993.
(17) Schnur, J. M. *Science* **1993**, *262*, 1669.
(18) Penner, R. M.; Martin, C. R. *J. Electrochem. Soc.* **1986**, *133*, 2206.
(19) Cai, Z.; Martin. C. R. *J. Am. Chem. Soc.* **1989**, *111*, 4138.
(20) Cai, Z.; Lei, J.; Liang, W.; Menon, V.; Martin, C. R. *Chem. Mater.* **1991**, *3*, 960.
(21) Liang, W.; Martin, C. R. *J. Am. Chem. Soc.* **1991**, *112*, 9666.
(22) Martin, C. R.; Parthasarathy, R. C.; Menon, V. *Synth. Met.* **1993**, *55*, 1165.
(23) Parthasarathy, R. V.; Martin, C. R. *Chem. Mater.* **1994**, *6*, 1627.
(24) Martin, C. R. *Science* **1994**, *266*, 1961.
(25) Martin, C. R. *Acc. Chem. Res.* **1995**, *28*, 957.

10.1021/cm020206u CCC: $22.00
Published on Web 07/24/2002

treatment of the template is required after polymerization.[16] Thus, nanostructures of conducting polymers, particularly nanotubes formed through a self-assembly process, are interesting at this time because they remain a scientific challenge. More recently, Huang and Wan[26] polymerized microtubules of polyaniline (PANI), using ammonium persulfate [$(NH_4)_2S_2O_8$, APS] as an oxidant in the presence of naphthalenesulfonic acid (NSA) as a dopant. This method was called a template-free method because no microporous membrane acting as a template was used. In particular, it was noted that NSA acted as a template in forming the PANI−NSA tubes;[27] however, the template did not need to be removed after polymerization because the NSA was acting as a dopant for PANI at the same time. Obviously, the new method is simple and inexpensive, compared with template synthesis, as this method omits the use of a microporous membrane as a template and the need for expensive equipment. Among conducting polymers, PANI has been extensively investigated because of its good processability and environmental stability and because its physical properties can be controlled by changing either the oxidation or the protonation state.[28−31] In particular, with respect to the protonic doping characteristics of PANI,[32] it is very interesting to synthesize nanostructures of PANI through a self-assembly process in the presence of sulfonic acid containing azobenzene as a dopant.

In this article, the synthesis and characterization of PANI nanostructures generated through a self-assembly process in the presence of azobenzenesulfonic acid (ABSA) as a dopant are reported for the first time. The resulting nanostructures of PANI−ABSA showed trans−cis photoisomerization similar to that of the azobenzene moiety upon irradiation by UV light ($\lambda = 365$ nm). The influence of synthesis conditions on the morphology, size, and electrical properties of the PANI−ABSA nanostructures was investigated, and their formation mechanism is discussed.

Experimental Section

The synthetic route to PANI doped with ABSA can be illustrated as follows:

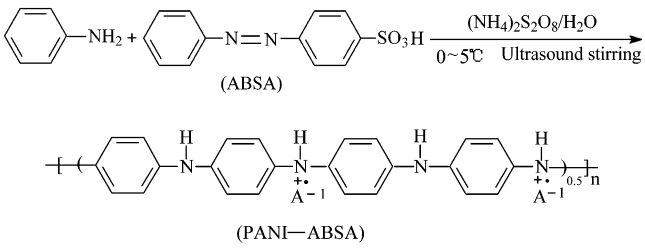

(26) Huang, J.; Wan, M. X. *J. Polym. Sci. A: Polym. Chem.* **1999**, *37*, 151.
(27) Wan, M. X. *Chin. J. Polym. Sci.* **1995**, *13*, 1.
(28) Angelopoulos, M,; Asturias, G. E.; Ermer, S. P.; Ray, A.; Scherr, E. M.; MacDiarmid, A. G. *Mol. Cryst. Liq. Cryst.* **1988**, *160*, 151.
(29) MacDiarmid, A. G.; Chiang, J. C.; Richter, A. F.; Epstein, A. J. *Synth. Met.* **1987**, 284.
(30) Lee, W. P.; Brenneman, K. R.; Hsu, C. H.; Shih, H.; Epstein, A. J. *Macromolecules* **2001**, *34* (8), 2648.
(31) Chaudhuri, D.; Kumar, A.; Rudra, I.; Sarma, D. D. *Adv. Mater.* **2001**, *13*(20), 1548.
(32) Zuo, F.; Angelopous, M.; MacDiarmid, G. A.; Epstein, J. A. *Phys. Rev. B* **1987**, *36*, 3475.

Table 1. XPS Analysis, Conductivity, and Morphology of PANI−ABSA Synthesized at Different [An]/[ABSA] Ratios

sample	An ($\times 10^{-3}$ mol)	ABSA ($\times 10^{-3}$ mol)	[An]/[ABSA]	conductivity (S/cm)	[S]/[N]	morphology
1	1.1	4.40	1:4	1.8	0.52	grain
2	1.1	2.20	1:2	3.9×10^{-1}	0.44	grain
3	11.0	1.10	10:1	2.6×10^{-2}	0.40	grain and flake
4	5.5	0.11	50:1	2.5×10^{-2}	0.38	tube and fiber
5	11.0	0.11	100:1	1.9×10^{-2}	0.36	grain and flake

where ABSA is represented by A. Aniline monomer was distilled under reduced pressure. ABSA (Shanghai Chemical Reagent Company) was recrystallized from ethanol/water solution (1:1). Ammonium persulfate [$(NH_4)_2S_2O_8$, APS] as an oxidant was used as received. Typical synthesis procedures for PANI−ABSA are as follows: One milliliter of aniline monomer mixed with 20 mL of ABSA aqueous solution (1.1×10^{-2} M) under ultrasound stirring for 1.0 h to obtain a uniform emulsion. To the above emulsion was quickly added 10 mL of an aqueous solution of APS (1.1 M) as an oxidant, and the mixture was kept at a temperature of 0−5 °C (in an ice bath) under ultrasound stirring for another 1 h. Then, the mixture was allowed to react at 0−5 °C for 9 h without stirring. The product was washed with deionized water, methanol, and diethyl ether several times and finally dried under vacuum for 24 h to obtain a dark-blue powder of PANI−ABSA.

The tubular morphology of PANI−ABSA was verified by scanning electron microscopy (SEM, JEOL JSM-6700F) and transmission electron microscopy (TEM, JEM-100CX II). Ultraviolet−visible (UV−vis) absorption spectra of ABSA and PANI−ABSA dissolved in *m*-cresol were recorded on a UV-3100 spectrometer. FTIR spectra (Perkin-Elmer system), ESR spectra (Bruker ER-200D), and X-ray diffraction data (MAC Science, Japan M-18AHF) were used to characterize the molecular structure of PANI−ABSA. The conductivity of powder pellets of PANI−ABSA at room temperature was measured by a four-probe method using a Keithley 196 System DMM digital mutimeter and an Advantest R6142 programmable dc voltage/current generator as the current source. The temperature dependence of the conductivity of the powder pellets of PANI−ABSA was measured by a standard four-probe method using a Keithley 220 programmable current source and 181 nanovoltmeter from 300 to 77 K. An ultraviolet lamp ($\lambda = 365$ nm, 8 W) was used as the light source for measuring trans−cis isomerization of ABSA and PANI−ABSA.

Results and Discussion

1. Morphology and Formation Mechanism. The effect of the synthetic conditions, such as the molar ratio of aniline to ABSA (represented by [An]/[ABSA]), the concentration of ABSA, the molar ratio of aniline to APS, and the reaction temperature, on the formation of PANI−ABSA nanostructures was investigated. It was found that the ratio of aniline to ABSA and the concentration of ABSA significantly affected the morphology of the resulting PANI−ABSA (Table 1). Figure 1 shows the influence of [An]/[ABSA] on the SEM images of PANI−ABSA. As one can see, irregular grains and flakes were observed when [An]/[ABSA] was equal to 1:1 or 10:1 (see Figure 1a and b). Interestingly, a regular fibrous morphology with a diameter of 110−130 nm and a length of 1−5 μm became dominant, when an aniline-to-ABSA ratio of 50:1 was used, as shown in Figure 1c. In particular, TEM image revealed that some of these fibers were hollow as nanotubes (Figure 2). When [An]/[ABSA] reached 100:1, however, irregular grains and flakes appeared again (Figure 1d). The above-described results indicate that a change in morphology of grains to tubes to grains took place as [An]/

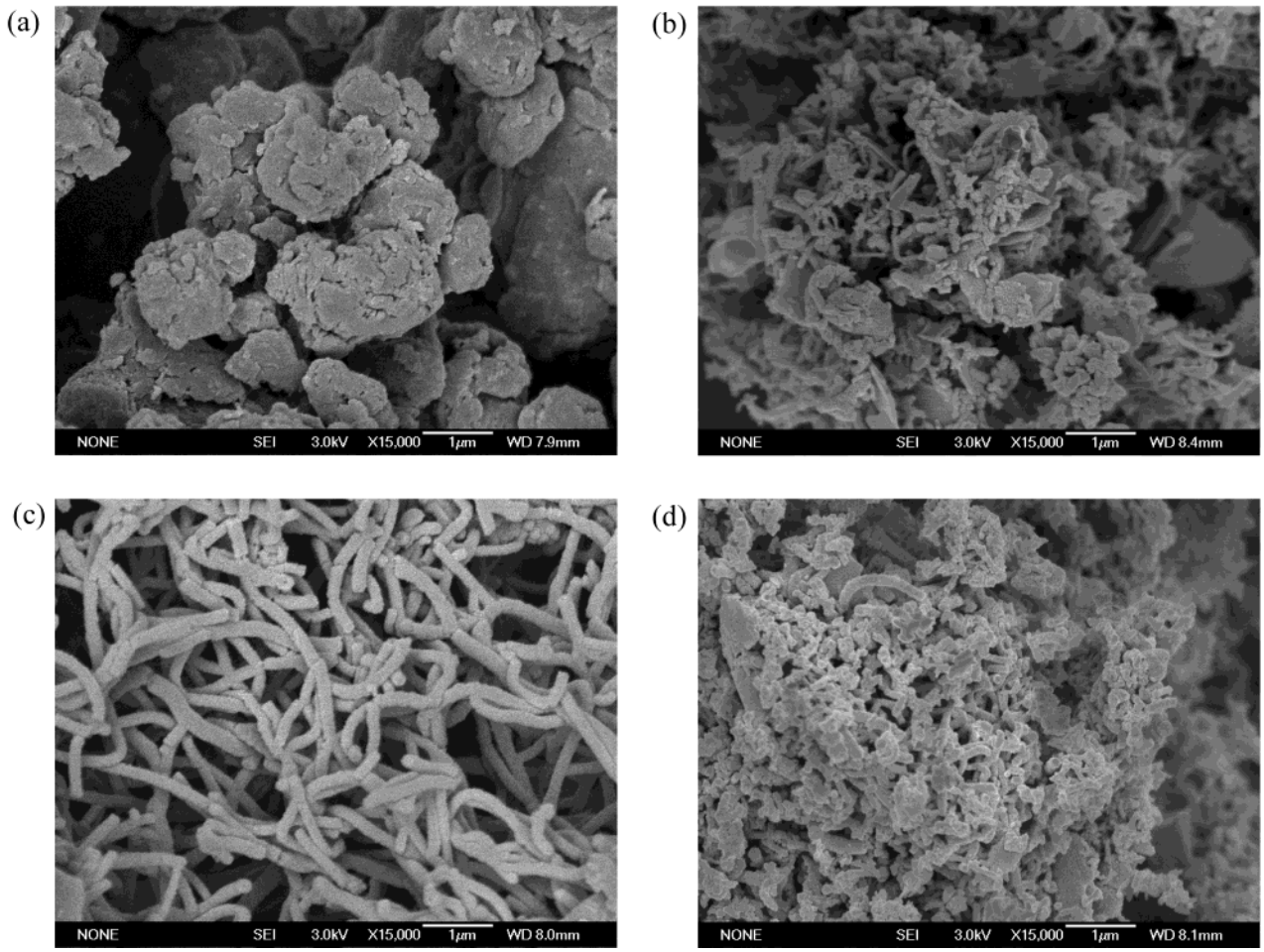

Figure 1. Influence of the molar ratio of aniline to ABSA on the morphology of PANI−ABSA: (a) 1:1, (b) 10:1, (c) 50:1, and (d) 100:1 (other reaction conditions: [APS] = 0.367 M, reaction time = 10 h, temp = 0−5 °C).

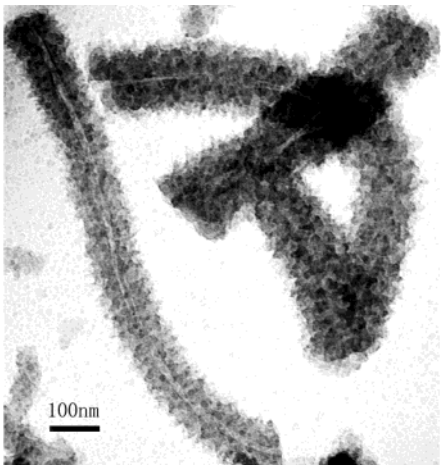

Figure 2. TEM image of PANI−ABSA nanotubes synthesized under the reaction conditions [An] = 0.367 M, [APS] = 0.367 M, [An]/[ABSA] = 50:1, reaction time = 10 h, temp = 0−5 °C.

[ABSA] varied from 1:1 to 100:1. We also found that the size of the PANI−ABSA nanotubes was strongly affected by the concentration of ABSA. Nanotubes with diameters of 30−60 nm and lengths of 3−8 μm were obtained, for example, when 1.1×10^{-3} M of ABSA was used. At higher concentrations of ABSA (e.g., 1.1×10^{-2} M), however, the diameter became larger (130−160 nm), and the length became smaller (1−3 μm). However, it was noted that effect of the molar ratio of aniline to APS and the reaction temperature on the morphology of PANI−ABSA nanotubes could be ignored.

To understand the formation mechanism of the PANI−ABSA nanotubes, SEM images of PANI−ABSA synthesized for different polymerization times were measured. As Figure 3 shows, PANI−ABSA exhibited a flake morphology (Figure 3a) when the polymerization time was about 5 min. After polymerization for 20 min, tubules mixed with flakes were observed (Figure 3b). Finally, the tubular morphology became dominant after polymerization for 1 h (see Figure 3c). The above-described results indicate that PANI−ABSA nanotubes might be formed by an aggregated process associated with the formation of micelles as templates. In fact, ABSA has both doping and surfactant functions because of the $-SO_3H$ group attached to the azobenzene moiety. According to our previous report,[33] it is expected that micelles formed by ABSA, or by anilinium cations, act as templates in the formation of PANI nanostructures. In addition, free aniline existing in the reaction solution might diffuse into the micelles to form micelles filled with free aniline that act as templates in the formation of PANI−ABSA nanofibers. Because APS as an oxidant is water-soluble, the polymerization reaction mainly takes place at the micelle−water interface.[34] In addition,

(33) Wei, Z. X.; Zhang, Z. M.; Wan, M. X. *Langmuir* **2002**, *18*, 917.
(34) Kim, B. J.; Oh, S. G.; Han, M. G.; Im, S. S. *Synth. Met.* **2001**, *122*, 297.

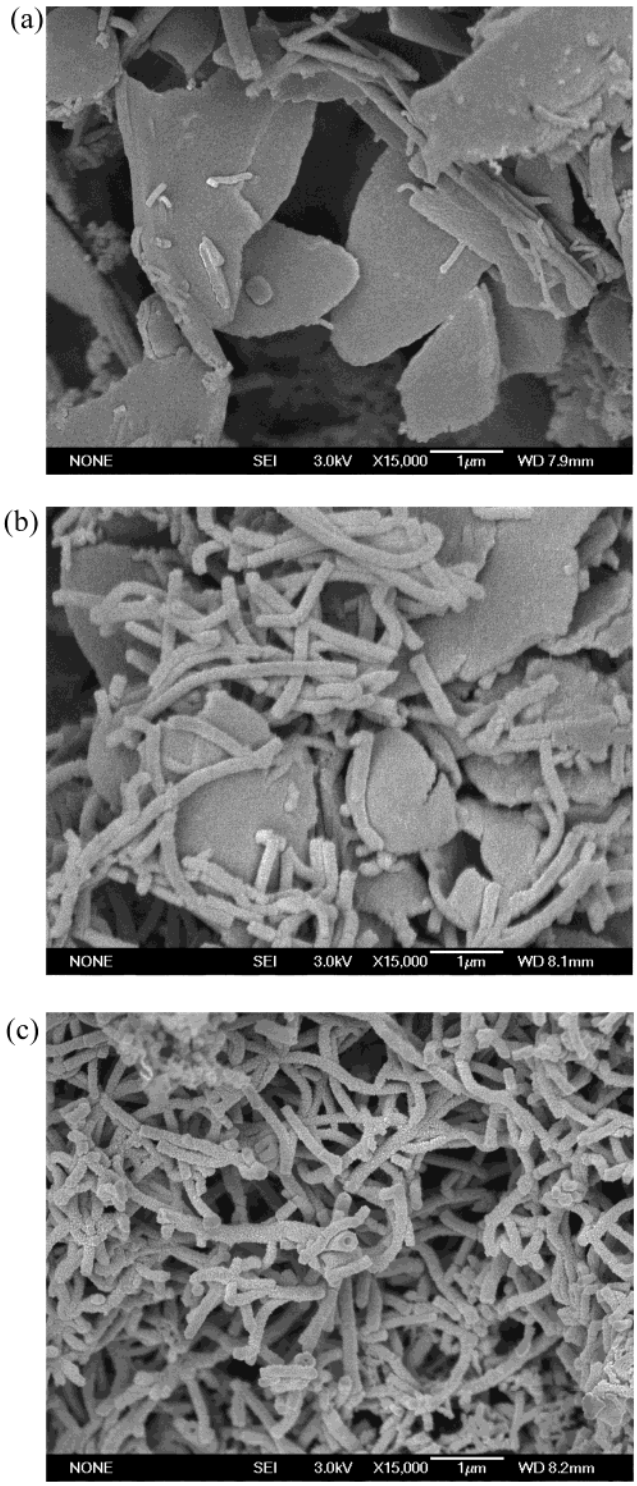

Figure 3. Effect of the polymerization time on SEM images of PANI−ABSA: (a) 5 min, (b) 20 min, (c) 1.0 h (other reaction conditions: [An] = 0.367 M, [APS] = 0.367 M, [An]/[ABSA] = 50:1, temp = 0−5 °C).

the contents of ABSA micelles, anilinium cations, and free aniline existing in the reaction solution are affected by the molar ratio of aniline to ABSA and the concentration of ABSA, resulting in variations in the morphology (hollow or solid) and size of the resulting PANI−ABSA nanostructures. These conclusions are consistent with our observations (Figures 1 and 3).

In addition, the formation of micelles is easily affected by the ionic strength of the solution. It was found that

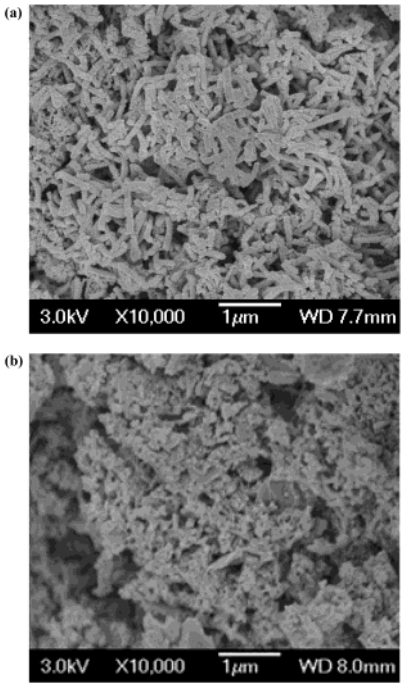

Figure 4. Influence of the NaCL concentration on the PANI−ABSA morphology: (a) [NaCL] = 0.037 M, (b) [NaCL] = 0.37 M (other reaction conditions: [An] = 0.367 M, [APS] = 0.367 M, [An]/[ABSA] = 50:1, temp = 0−5 °C).

short PANI−ABSA nanotubes that are 70−100 nm in diameter and 0.4−1.0 μm in length were obtained when 3.7×10^{-2} M NaCL was added, as shown Figure 4a. In particular, the PANI−ABSA structures became grains upon the addition of higher concentrations of NaCL (e.g., 3.7×10^{-1} M) (Figure 4b). Up to now, it has been proposed that the formation of PANI−ABSA nanostructures might be due to self-assembly of the ABSA and /or anilinium cations into a nanostructural intermediate[35,36] that acts as both a supermolecular template[37] and a self-doping reagent.

2. Photochromism of ABSA and PANI−ABSA. UV−vis absorption spectra of ABSA and PANI−ABSA dissolved in *m*-cresol solution were measured, as shown in Figures 5 and 6, respectively. Two bands at about 330 and 440 nm were observed in the UV−vis absorption spectrum of ABSA (see Figure 5). The first absorption band corresponds to the $\pi-\pi^*$ transition of the azobenzene moiety, while the latter is assigned as the $n-\pi^*$ transition of the azobenzene moiety. These assignments are in agreement with those of the model compound azobenzene.[38] For PANI−ABSA nanotubes, on the other hand, three bands at about 330, 430, and 800 nm were observed (see Figure 6). The band around 330 nm can be attributed to the overlap of the $\pi-\pi^*$ transition of the benzoid rings of PANI and the azobenzene moiety.[39] The band at about 430 nm is related to the $n-\pi^*$ transition of the azobenzene moiety.[38] One piece of evidence supporting this conclusion is that the

(35) Wan, M. X.; Shen, Y. Q.; Huang, J. Chinese Patent 98109916.5, 1998.
(36) Wan, M. X.; Li, J. C. *J. Polym. Sci. A: Polym. Chem.* **2000**, *38*, 2359.
(37) Beginn, U. *Adv. Mater.* **1998**, *10*, 1391.
(38) Tamai, N.; Hiroshi, M. *Chem. Rev.* **2000**, *100*, 1875.
(39) Yang, S. C.; Cushman, R. J.; Zhang, D. *Synth. Met.* **1992**, *48*, 24.

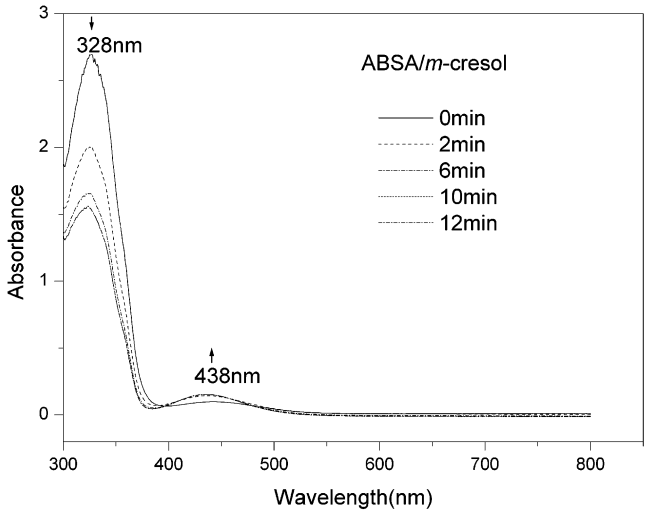

Figure 5. UV−vis spectra of ABSA dissolved in *m*-cresol solution upon UV irradiation (λ = 365 nm).

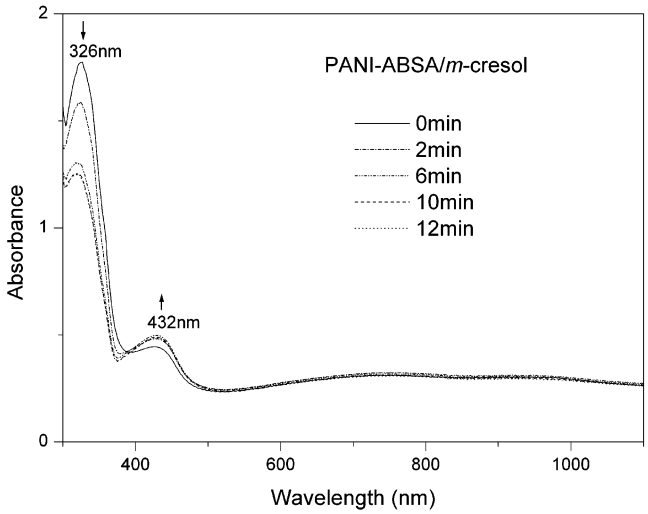

Figure 6. UV−vis spectra of PANI−ABSA nanotubes dissolved in *m*-cresol solution upon UV irradiation (λ = 365 nm).

photoinduced isomerization of PANI−ABSA was observed at 430 nm (see Figure 6), while the photoinduced isomerization for common PANI was absent, although a band at 420 nm can be observed in the spectrum of doped PANI.[39] The band at about 800 nm with a long tail is assigned to the polaron transition, which is a typical protonation characterization, identical to that of the emeraldine salt form of PANI.[40]

As shown in Figure 5, the absorption intensity at about 330 nm for ABSA significantly decreased, and that at about 440 nm increased upon irradiation with ultraviolet light (λ = 365 nm). These results are identical to those obtained for trans−cis isomerization of the azobenzene moiety.[1] In particular, a similar isomerization for PANI−ABSA nanotubes was also observed, as shown in Figure 6. Thus, it is reasonable to believe that the observed photoinduced isomerization of PANI−ABSA nanotubes can be attributed to the isomerization characteristics of the azobenzene moiety. To further understand the characteristics of the photoinduced

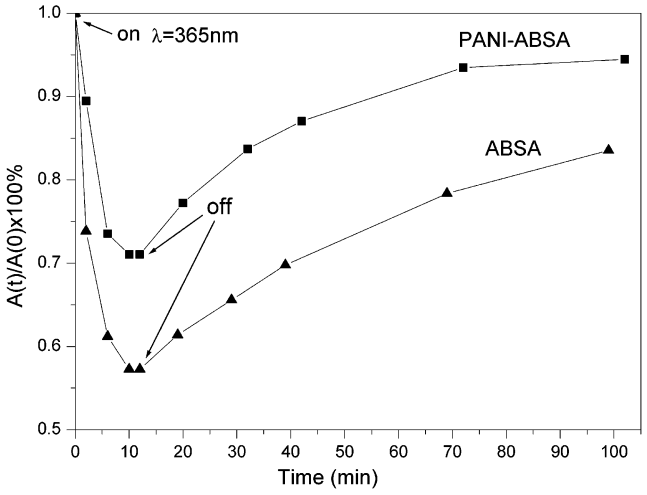

Figure 7. Kinetics of the photoisomerization of ABSA and PANI−ABSA dissolved in *m*-cresol solution.

isomerization of PANI−ABSA nanotubes, the kinetics of the photoisomerization of ABSA and PANI−ABSA dissolved in *m*-cresol were measured, as shown in Figure 7. It was found that the intensity of the band at 330 nm for ABSA decreased immediately to 57.3% of the initial value after irradiation with UV light for 10 min; then, the absorption slowly recovered in visible light, corresponding to cis−trans isomerization. The absorption of this band reverted to 83.4% of the initial value after the UV light had been switched off for 100 min. A similar photoisomerization process was observed for PANI−ABSA (see Figure 7). As Figure 7 shows, the rate of photoisomerization of PANI−ABSA is reduced in comparison to that of ABSA. However, the recovery of PANI−ABSA exhibits a synchronization process with ABSA. These results suggest that the doped *trans*-azobenzene moieties along the backbone, probably owing to steric hindrance, are more resistant to the photoisomerization process. However, the absence of a pronounced effect on the *trans*-azobenzene photoinduced isomerization rate of ABSA and PANI−ABSA indicates that the photoisomerization mechanism might involve an in-plane translation of the benzene ring further from the main chain rather than rotation about the N=N bond, as previously proposed.[41−43]

3. Structural Characterization of PANI−ABSA. We used FTIR spectroscopy and X-ray diffraction to characterize the molecular structure of PANI−ABSA, in particular PANI−ABSA nanotubes synthesized at [An]/[ABSA] = 50:1. The FTIR spectrum shows that all characteristic bands of PANI at the 1583 cm^{-1} (assigned as C=C stretching of the quinoid rings), 1496 cm^{-1}(C=C stretching of benzenoid rings), 1300 cm^{-1} (C−N stretching mode) and 1140 cm^{-1} (N=Q=N, where Q represents the quionoid ring) were observed in the FTIR spectra of PANI−ABSA (see Figure 8). This indicatesthat the spectrum of nanotubes is identical to the emeraldine salt form of PANI.[44]

(40) Salaneck, W. R.; Liedberg, B.; Inganäs, O.; Erlandsson, R.; Lundström, I.; MacDiarmid, A. G.; Halpern, M.; Somasiri, N. L. D. *Mol. Cryst. Liq. Cryst.* **1985**, *121*, 191.

(41) Talaty, E. R.; Fargo, J. C. *Chem. Commun.* **1967**, 65.

(42) Haberfield, P.; Block, P. M.; Lux, S. M. *J. Am. Chem. Soc.* **1975**, *97*, 5804.

(43) Nerbonne, J. M.; Weiss, R. J. *J. Am. Chem. Soc.* **1978**, *100*, 5953.

(44) Tang, J. S.; Jing, X. B.; Wang, B. C.; Wang, F. S. *Synth. Met.* **1988**, *24*, 231.

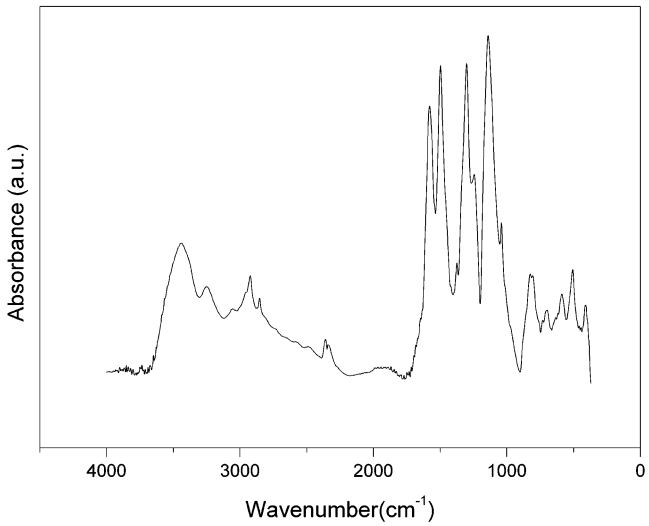

Figure 8. FTIR spectra of PANI−ABSA nanotubes synthesized under the reaction conditions [An] = 0.367 M, [APS] = 0.367 M, [An]/[ABSA] = 50:1, reaction time = 10 h, temp = 0−5 °C.

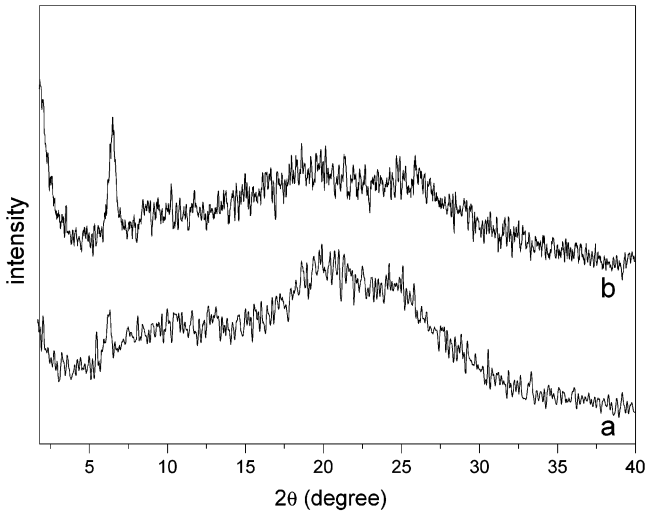

Figure 9. X-ray scattering patterns of PANI−ABSA with different morphologies: (a) grains, (b) tubes. For a, [An]/[ABSA] = 10:1; for b, [An]/[ABSA] = 50:1 (other reaction conditions: [An] = 0.367 M, [APS] = 0.367 M, reaction time = 10 h, temp = 0−5 °C).

The X-ray diffraction patterns of PANI−ABSA with different morphologies are shown in Figure 9. The XRD data were amorphous. However, a narrow peak centered at $2\theta = 6.5$ was observed that might be related to the limited short-range order.[45] In particular, this peak of PANI−ABSA nanotubes was sharper than that of PANI−ABSA grains, which can be attributed to a tubular morphology.

4. Electrical Properties of PANI−ABSA. The conductivity of PANI−ABSA at room temperature is closely related to the [An]/[ABSA] ratio, as indicated by the results given in Table 1. As can be seen, when [An]/[ABSA] changed from 1:4 to 100:1, for example, the conductivity dropped dramatically by 2 orders of magnitude. This was due to the different degrees of doping (denoted by the ratio [S]/[N]) measured by XPS (Table 1).

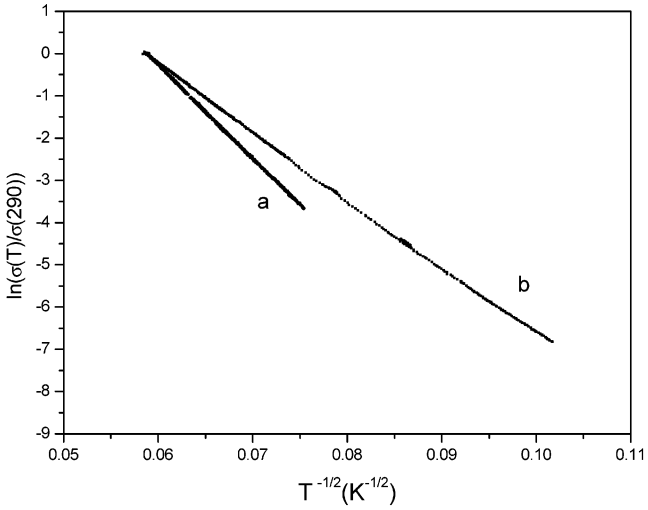

Figure 10. Temperature dependence of the conductivity for PANI−ABSA with different morphologies: (a) grains, (b) tubes. For a, [An]/[ABSA] = 10:1; for b, [An]/[ABSA] = 50:1 (other reaction conditions: [An] = 0.367 M, [APS] = 0.367 M, reaction time = 10 h, temp = 0−5 °C).

The temperature dependence of the conductivity of PANI−ABSA exhibits a typical semiconductor behavior that can be expressed according to variable-range hopping (VRH) model proposed by Mott[46] as follows

$$\sigma(T) = \sigma_0 \exp[-(T_0/T)^{1/(n+1)}] \quad n = 1, 2, 3$$

$$T_0 = 8\alpha/ZN(E_F)K_B$$

where α^{-1} is the localization length, $N(E_F)$ is the density of states at the Fermi level, K_B is the Boltzmann constant, and Z is the number of nearest-neighbor chains. All data are in agreement with the one-dimensional VRH (1D-VRH) model ($n = 1$). By plotting ln $\sigma(T)/\sigma(290)$ vs $T^{-1/2}$, as shown in Figure 10, the T_0 value corresponding to the required energies of charge carriers can be obtained from the slope of the straight line. The T_0 value of PANI−ABSA nanotubes (2.6×10^4 K) is slightly lower than that of PANI−ABSA grains (4.9×10^4 K), which is consistent with the results obtained from room-temperature conductivity measurements.

Conclusion

Nanotubes and nanofibers of polyaniline (PANI) with a diameter of 110−130 nm and a conductivity of 2.5×10^{-2} S/cm were synthesized through a self-assembly process in the presence of ABSA as a dopant. It was found that the formation and size of the PANI−ABSA nanostructures strongly depended on the aniline-to-ABSA ratio and on the concentration of ABSA. The micelles formed by ABSA or anilinum cations act as templates in the formation of PANI−ABSA nanostructures. In particular, the resulting PANI−ABSA nanostructures exhibited trans−cis photoisomerization upon irradiation with UV light (λ = 365 nm), which is attributed to the azobenzene moiety of the ABSA dopant.

(45) (a) Ginder, J. M.; Ritchter, A. H.; MacDiarmid, A. G.; Epstein, J. A.; *J. Solid. State Commun.* **1987**, *63*, 97. (b) Zuo, F.; Angelopoulos, M.; Macdiarmid, A. G.; Epstein, J. A. *Phys. Rev. B.* **1987**, *36*, 3475.

(46) Mott, N. F.; Davis, E. A. *Electronic Processes in Noncrystalline Materials*; Clarendon Press: Oxford, U.K., 1979.

Acknowledgment. This project was supported by the National Natural Science Foundation of China (29974037 and 50133010) and the Center for Molecular Sciences, Institute of Chemistry, Chinese Academy of Sciences (CMS-CX2001). We also thank Prof. Zhaojia Chen for measurements of the temperature dependence of conductivity.

CM020206U